



Citation for published version:

Shaharum, NSN, Shafri, HZM, Ghani, WAWAK, Samsatli, S, Al-Habshi, MMA & Yusuf, B 2020, 'Oil Palm Mapping Over Peninsular Malaysia Using Google Earth Engine and Machine Learning Algorithms', *Remote Sensing Applications: Society and Environment*, vol. 17, 100287. <https://doi.org/10.1016/j.rsase.2020.100287>

DOI:

[10.1016/j.rsase.2020.100287](https://doi.org/10.1016/j.rsase.2020.100287)

Publication date:

2020

Document Version

Peer reviewed version

[Link to publication](#)

Publisher Rights

CC BY-NC-ND

University of Bath

Alternative formats

If you require this document in an alternative format, please contact:
openaccess@bath.ac.uk

General rights

Copyright and moral rights for the publications made accessible in the public portal are retained by the authors and/or other copyright owners and it is a condition of accessing publications that users recognise and abide by the legal requirements associated with these rights.

Take down policy

If you believe that this document breaches copyright please contact us providing details, and we will remove access to the work immediately and investigate your claim.

Manuscript Details

Manuscript number	RSASE_2019_318_R1
Title	Oil Palm Mapping Over Peninsular Malaysia Using Google Earth Engine and Machine Learning Algorithms
Article type	Research Paper

Abstract

Oil palm plays a pivotal role in the ecosystem, environment, economy and without proper monitoring, uncontrolled oil palm activities could contribute to deforestation that can cause high negative impacts on the environment and therefore, proper management and monitoring of the oil palm industry are necessary. Mapping the distribution of oil palm is crucial in order to manage and plan the sustainable operations of oil palm plantations. Remote sensing provides a means to detect and map oil palm from space effectively. Recent advances in cloud computing and big data allow rapid mapping to be performed over large a geographical scale. In this study, 30 m Landsat 8 data were processed using a cloud computing platform of Google Earth Engine (GEE) in order to classify oil palm land cover using non-parametric machine learning algorithms such as Support Vector Machine (SVM), Classification and Regression Tree (CART) and Random Forest (RF) for the first time over Peninsular Malaysia. The hyperparameters were tuned, and the overall accuracy produced by the SVM, CART and RF were 93.16%, 80.08% and 86.50% respectively. Overall, the SVM classified the 7 classes (water, built-up, bare soil, forest, oil palm, other vegetation and paddy) the best. However, RF extracted oil palm information better than the SVM. The algorithms were compared and the McNemar's test showed significant values for comparisons between SVM and CART and RF and CART. On the other hand, the performance of SVM and RF are considered equally effective. Despite the challenges in implementing machine learning optimisation using GEE over a large area, this paper shows the efficiency of GEE as a cloud-based free platform to perform bioresource distributions mapping such as oil palm over a large area in Peninsular Malaysia.

Keywords cloud computing; Landsat; oil palm

Corresponding Author Helmi Shafri

Corresponding Author's Institution Universiti Putra Malaysia (UPM)

Order of Authors Nur Shafira Nisa Shaharum, Helmi Shafri, Wan Azlina Wan Ab Karim Ghani, Sheila Samsatli, Mohammed Al-Habshi, Badronnisa Yusuf

1
2
3
4
5
6
7
8
9
10
11
12
13

Oil Palm Mapping Over Peninsular Malaysia Using Google Earth Engine and Machine Learning Algorithms

14
15
16
17
18
19
20
21
22
23
24
25
26
27
28
29
30
31
32
33
34
35
36
37
38
39
40
41
42
43
44
45
46
47
48
49
50
51
52
53
54
55
56
57
58
59

Nur Shafira Nisa Shaharum^a, Helmi Zulhaidi Mohd Shafri^{a,b*}, Wan Azlina Wan
Ab Karim Ghani^c, Sheila Samsatli^d, Mohammed Mustafa Abdulrahman Al-
Habshi^a and Badronnisa Yusuf^a

^aDepartment of Civil Engineering, Faculty of Engineering, Universiti Putra Malaysia, 43400, UPM Serdang, Selangor, Malaysia; ^bGeospatial Information Science Research Centre (GISRC), Faculty of Engineering, Universiti Putra Malaysia (UPM), 43400 Serdang, Selangor, Malaysia; ^cDepartment of Chemical and Environmental Engineering/Sustainable Process Engineering Research Centre (SPERC), Faculty of Engineering, Universiti Putra Malaysia, 43400, UPM Serdang, Selangor, Malaysia; ^dDepartment of Chemical Engineering, University of Bath, Claverton Down, BA2 7AY, United Kingdom.

Corresponding author: helmi@upm.edu.my

Oil Palm Mapping Over Peninsular Malaysia using Google Earth Engine and Machine Learning Algorithms

Abstract

Oil palm plays a pivotal role in the ecosystem, environment, economy and without proper monitoring, uncontrolled oil palm activities could contribute to deforestation that can cause high negative impacts on the environment and therefore, proper management and monitoring of the oil palm industry are necessary. Mapping the distribution of oil palm is crucial in order to manage and plan the sustainable operations of oil palm plantations. Remote sensing provides a means to detect and map oil palm from space effectively. Recent advances in cloud computing and big data allow rapid mapping to be performed over large a geographical scale. In this study, 30 m Landsat 8 data were processed using a cloud computing platform of Google Earth Engine (GEE) in order to classify oil palm land cover using non-parametric machine learning algorithms such as Support Vector Machine (SVM), Classification and Regression Tree (CART) and Random Forest (RF) for the first time over Peninsular Malaysia. The hyperparameters were tuned, and the overall accuracy produced by the SVM, CART and RF were 93.16%, 80.08% and 86.50% respectively. Overall, the SVM classified the 7 classes (water, built-up, bare soil, forest, oil palm, other vegetation and paddy) the best. However, RF extracted oil palm information better than the SVM. The algorithms were compared and the McNemar's test showed significant values for comparisons between SVM and CART and RF and CART. On the other hand, the performance of SVM and RF are considered equally effective. Despite the challenges in implementing machine learning optimisation using GEE over a large area, this paper shows the efficiency of GEE as a cloud-based free platform to perform bioresource distributions mapping such as oil palm over a large area in Peninsular Malaysia.

Keywords: cloud computing; image classification; Landsat; machine learning; oil palm

1. Introduction

Malaysia is a Southeast Asian country sharing borders with Thailand, Indonesia and Brunei.

Malaysia is a tropical country with two geographical regions: Peninsular Malaysia and

Borneo (Sabah and Sarawak). It experiences a humid, hot and rainy climate throughout the year, experiencing temperature ranging between 23°C – 32°C throughout the country. This

119
120
121 allows Malaysia to generate income from agricultural crop activities such as paddy
122
123 cultivation, rubber and oil palm planting (Fahmi et al. 2013; Nambiappan et al. 2018). Among
124
125 the agricultural crops, oil palm produces the highest amount of biomass, and as one of the
126
127 largest palm oil exporters in the world, the total number oil palms planted in Malaysia
128
129 reached over 5 million hectares (ha) in 2017 (Ng et al. 2012). Moreover, oil palm was the
130
131 main contributor of agricultural crops to the country's GDP in 2017 with a total contribution
132
133 of 46.6% (Mahidin 2018). Despite its benefits, oil palm activities contributed to massive
134
135 deforestation and caused negative impacts to the environment (Fitzherbert et al. 2008) and
136
137 therefore, oil palm activities have been labelled as the main threat to the earth by contributing
138
139 to the global warming and climate change (Shuit et al. 2009). Destroying wildlife habitats and
140
141 forests for planting oil palm trees have worsened the negative implications. Even though
142
143 palm oil can be used as a renewable energy source and help contribute to the 17 Sustainable
144
145 Development Goals as presented by the United Nations, it is important to note that the
146
147 environment will be in jeopardy without proper management and monitoring on the oil palm
148
149 industry, which will in turn affect environmental sustainability. However, managing huge
150
151 areas of oil palm plantations will be challenging. Furthermore, implementing ground surveys
152
153 or other traditional survey methods will require a tremendous amount of time, effort and high
154
155 cost. A number of people are required to execute data collection over a large area and
156
157 therefore, high computational power will be essential to process such big data. Hence, the
158
159 utilisation of remote sensing is a suitable and a cost-effective method for collecting data
160
161 covering a huge area.
162
163
164

165
166 The use of remote sensing for oil palm applications can be found in many publications
167
168 using a variety of sensors, platforms and algorithms. For example, Thenkabail et al. (2004)
169
170 used four bands with 4 m of spatial resolution from IKONOS to carry out a study on oil palm
171
172 biomass estimations and carbon stock calculations. Before implementing image
173
174
175
176
177

178
179
180 classification, the band was first masked by extracting the oil palm feature from non-oil

181
182 palms. Next, Gutiérrez-Vélez and DeFries (2013) utilised MODIS data with 250 m of pixel
183 size and successfully produced an oil palm map covering an area of 939,204 km². Another
184 similar study using MODIS data was conducted on a larger study area covering several
185 regions in Southeast Asia including Peninsular Malaysia, Sumatra, Java, Borneo, Sulawesi
186 and Mindanao. The study has successfully classified a total of 13 classes together with
187 mangrove forests, rainforests and large-scale palm plantations (Miettinen et al. 2012). This
188 indicated that studies using coarse spatial resolution can be implemented in oil palm studies.
189 On the other hand, using higher spatial resolution data, analysis on oil palm studies can be
190 improved and more information can be extracted. Jusoff and Pathan (2009) and Shafri and
191 Hamdan (2009) used hyperspectral sensor to map individual oil palm trees. A more subtle
192 analysis was conducted by Shafri et al. (2011) via Maximum Likelihood Classifier (MLC)
193 and successfully detected Ganoderma disease infections in the plantations with an overall
194 accuracy of 82%. More recently, the high spectral resolution as provided by hyperspectral
195 data has allowed Camacho et al. (2019) to successfully produce an oil palm map
196 distinguishing healthy from diseased palm trees.
197
198
199
200
201
202
203
204
205
206
207
208
209
210
211
212
213

214 In terms of classification algorithms, Morel et al. (2012) have successfully
215 distinguished between forest and oil palm areas on Landsat data using k-means and MLC
216 algorithms. Then, Glinskis and Gutiérrez-Vélez (2019) used MLC algorithm to classify oil
217 palm and successfully categorised it into 3 stages (infant palm, juvenile palm and adult palm)
218 via Sentinel 1 and 2 data. Studies using more advanced algorithms or approaches such as
219 Support Vector Machine (SVM), Random Forest (RF), Deep Learning, Artificial Neural
220 Network (ANN) and other machine learning algorithms to classify oil palm land cover tend to
221 produce better results (Nooni et al. 2014; Li et al. 2015; Lee et al. 2016; Noi and Kappas
222 2018). For example, Cheng et al. (2016) performed land cover classifications on Landsat and
223
224
225
226
227
228
229
230
231
232
233
234
235
236

237
238
239 ALOS-PALSAR remote sensing data via SVM and Minimum Distance algorithms. The
240
241 classifications were applied on two different sites, and the overall accuracies produced by
242
243 SVM were higher than Minimum Distance for both Landsat and ALOS-PALSAR data.
244
245 Cheng et al. (2018) expanded the oil palm classification on larger areas covering Malaysia,
246
247 Indonesia, Thailand, Nigeria and Ghana using ALOS-PALSAR data. The study achieved an
248
249 overall accuracy of more than 94% for all the aforementioned countries. **A review of studies**
250
251 **on fusion techniques between optical and radar data to map land use was conducted by Joshi**
252
253 **et al (2016) and it showed that fusion techniques are efficient for cloud issue. De Alban et al**
254
255 **(2018) combined Landsat and L-band Synthetic Aperture Radar (SAR) data to carry out land**
256
257 **use land cover change application in tropical landscapes. A machine learning RF algorithm**
258
259 **was used to classify the land use and the accuracy obtained was 92.96% to 93.83%. However,**
260
261 **fusion technique requires large amount of time and data to produce the cloud-free image.**
262
263

264
265 As shown above, there have been several oil palm studies using various remote
266
267 sensing data, however, most of the studies were limited to small areas (Li et al. 2016; Chong
268
269 et al. 2017; Charters et al. 2019; Fawcett et al. 2019) and utilised personal computers,
270
271 requiring the ability to store data and perform image processing using remote sensing
272
273 software that were mostly commercial. Data obtained from the impacts of oil palm activities
274
275 that were conducted on small areas are not suitable and insufficient to be used for measuring
276
277 the sustainability level for a huge area, especially for the whole country. On the other hand,
278
279 the utilisation of very high-resolution images on big areas will be costly in addition to
280
281 requiring high computational power which will be essential to process the data. Even so, GEE
282
283 cloud computing provides an alternative to process huge amount of geospatial data with zero
284
285 cost and without the need to personally store the data on the personal computer. Sidhu et al.
286
287 (2018) performed land cover change analysis in Singapore's landmass via GEE and the result
288
289 showed that the forest cover was affected by the monsoon cycles. Another study by Oliphant
290
291
292
293
294
295

296
297
298 et al. (2019) to map cropland over Southeast and Northeast Asia via Landsat was carried out
299
300 using GEE, but no specific crops (e.g. oil palm, paddy and others) are mapped. In Malaysia,
301
302 first ever effort to map oil palm over the Peninsular Malaysia using cloud computing platform
303
304 was done using the Remote Ecosystem Monitoring Assessment Pipeline (REMAP) tool as
305
306 conducted by Shaharum et al. (2019). However, it was limited to only the use of RF
307
308 classifier, limiting the investigation of the performance of other machine learning algorithms.
309
310 Furthermore, as the toolbox is not programmable, the parameters of the classifier cannot be
311
312 optimized or tuned accordingly. In addition, the imagery data used in REMAP was fixed and
313
314 cannot be filtered to produce the best cloud-free data. In addition, the GEE algorithms were
315
316 run in code editor module, allowing more optimization parameters to be tested for
317
318 classification. To the best of our knowledge, there has been no report on the utilisation of
319
320 GEE for oil palm mapping over the entire Peninsular Malaysia. Hence, this study was
321
322 conducted to test the capability of 30 m Landsat data using the GEE cloud computing
323
324 platform and compare machine learning algorithms such as SVM, CART and RF to map oil
325
326 palm land cover over Peninsular Malaysia covering an area of 132,265 km². Even though
327
328 there are many available remote sensing data and techniques available to classify the oil palm
329
330 plantation, selecting the best technique will be vital.
331
332
333

334 335 **2. Material and Methods**

336 337 **2.1 Study area**

338
339 Malaysia is located between Thailand, Singapore and Indonesia. It comprises of two regions:
340
341 Peninsular Malaysia and Borneo (Sabah and Sarawak). This study covers Peninsular
342
343 Malaysia (N 4°00'0.00", E 102°29'59.99"; Fig 1) or West Malaysia with an approximate land
344
345 area of 132,265 km². Malaysia is a tropical country experiencing both hot and humid weather
346
347
348
349
350
351
352
353
354

355
356
357 throughout the year. The temperature ranges between 23°C – 32°C and during hot weather,
358
359 the temperature can exceed over 40°C (Shahar 2016).
360
361
362
363

364
365
366 [Figure 1 near here]
367
368

369 **2.2 Google Earth Engine**

370
371
372 Vast amount of the geospatial remote sensing data provided in the GEE has allowed the
373
374 powerful cloud-based platform to be used in various studies involving deforestation, oil palm
375
376 plantations, environmental assessment, change detection and urban classifications (Patel et al.
377
378 2015; Dong et al. 2016; Goldblatt et al. 2016; Shelestov et al. 2017). GEE can be accessed
379
380 either through Application Programming Interface (API) or web-based Interactive
381
382 Development Environment (IDE) (Gorelick et al. 2017). The data catalog provided in the
383
384 GEE houses a multi-petabyte accessible geospatial dataset that is made up of Earth-observing
385
386 remote sensing images, including Landsat, MODIS, Sentinel-1 and Sentinel-2.
387
388
389
390
391

392 [Figure 2 near here]
393
394
395

396
397 Figure 2 shows the GEE platform via Javascript API and it allows the user to control the data
398
399 through coding. The user can write the programs using client libraries in Python and
400
401 Javascript (programming languages). Furthermore, the client libraries provide objects for
402
403 Images, Collections and other data types. In fact, the user can perform various remote sensing
404
405 analyses in the GEE API platform such as image classifications, multitemporal urban extents,
406
407 post-processing and object detection. Enormous amount of Earth Engine public data catalog
408
409 provided in the cloud-based GEE platform helps the user to process very large geospatial
410
411
412
413

414
415
416 datasets without having to suffer the information technology pains including the need of high
417
418 computational power resources and huge amount of storage.
419
420
421
422

423 **2.3 Data collection and pre-processing**

424
425
426
427 The availability of 30 m Landsat 8 images for the study area were obtained from the United
428 States Geological Survey through the GEE platform (Roy et al. 2014). The images were
429 already being pre-processed and corrected at Top-Of-Atmosphere (TOA) reflectance as
430 explained by Chander et al. (2009) by converting at sensor (spectral radiance) to
431 exoatmospheric TOA reflectance. The benefits of using images that have been corrected at
432 TOA reflectance are it compensates for different values of the exoatmospheric solar
433 irradiance occur from spectral band differences and the TOA reflectance can eliminate the
434 cosine effect of different solar zenith angles due to the time difference between data
435 acquisitions. Also, it corrects the dissimilarity in the Earth–Sun distance between different
436 data acquisition dates.
437
438
439
440
441
442
443
444
445
446
447
448
449
450

451 [Table 1 near here]
452
453
454
455

456 This study utilised only 7 bands of Landsat 8 with 30 m spatial resolution (see Table 1).
457 Landsat 8 data is obtained via passive remote sensing, and it is sensitive towards clouds.
458 Several Landsat 8 images taken from year 2016 and 2017 were patched together to attain the
459 missing information that were blocked by the clouds. The existence of clouds can affect the
460 quality of the remote sensing data and furthermore, the information beneath the cloud will be
461 unclassified. The utilisation of commercial remote sensing software to perform image
462 patching on a huge area consumes significant resources and time (Gambo et al. 2018;
463
464
465
466
467
468
469
470
471
472

473
474
475 Shaharum et al. 2018). However, the GEE platform allows the user to perform data
476
477 acquisition and image patching in a few seconds. Furthermore, it allows the user to set the
478
479 percentage of the cloud cover and the desired date of the satellite data to be used.
480
481

482 **3. Methodology**

483
484
485 Several geospatial datasets were utilised in this study to produce the oil palm land cover maps
486
487 over Peninsular Malaysia: (i) 30 m Landsat 8 data from 2016 to 2017 (7 original bands) (ii)
488
489 Shuttle Radar Topographic Mission (SRTM), Digital Elevation Model (DEM), (iii)
490
491 Additional data including NDVI, Normalised Difference Water Index (NDWI) and others.
492
493
494 The workflow adapted for this study is shown in Figure 3.
495
496

497 [Figure 3 near here]
498

499
500 This study compared 3 different machine learning algorithms (SVM, RF and CART), and a
501
502 total of 7 classes including oil palm were classified. The importance of oil palm plantation
503
504 has been discussed in the introduction and therefore, this study focuses on producing oil palm
505
506 land cover map. Moreover, the land cover map produced can later be used in the next study to
507
508 assess the impacts of oil palm plantation over Peninsular Malaysia.
509
510

511 **3.1 Data used for classification**

512
513
514 As illustrated in Table 1, a total of 7 bands obtained from Landsat 8 images were used and
515
516 these bands were used to generate additional data (see Table 2). A number of equations were
517
518 used to produce additional data that will be included together with the other 7 bands to be
519
520 used in the image classification stage.
521
522

523 [Table 2 near here]
524
525
526
527
528
529
530
531

532
533
534 The layers in Table 2 were stacked together with Landsat 8 bands (Table 1) to be used in the
535 classification process. These additional layers are capable of extracting a certain information
536 in a more efficient way. For example, NDVI is derived from the ratio between Red and Near-
537 infrared (NIR) reflectance bands. Furthermore, NDVI is sensitive towards chlorophyll
538 content and the green leaf density. The presence of chlorophyll in green vegetations absorbs
539 in the red band. Hence, NDVI is useful to extract information of the green vegetations on the
540 ground (Bro-Jørgensen et al. 2008).
541
542
543
544
545
546
547
548
549
550
551

552 **3.2 Sampling**

553
554 Samples were created in the GEE platform and a total of 7 classes were identified: water,
555 built-up, bare soil, oil palm, forest, other vegetation and paddy. The samples were created
556 using the point format for every state in Peninsular Malaysia, covering a total of 11 states via
557 random sampling. The samples were created with the aid of land cover map provided by the
558 Department of Agriculture (DOA) and high-resolution Google Earth images as shown in
559 Figure 4(a). The samples were then divided into two components: training and testing. A total
560 of 70% from the whole created samples (4307 points) were used to classify the Landsat
561 images and the remaining 30% of the samples (1846 points) were used to validate and assess
562 the accuracy of the algorithms used. The classification and validation were done in GEE and
563 the accuracy assessment was calculated using the common confusion matrix method.
564
565
566
567
568
569
570
571
572
573
574
575
576
577
578

579 [Figure 4 near here]
580
581
582
583
584
585
586
587
588
589
590

3.3 Supervised machine learning algorithms

3.3.1 Support Vector Machine

Supervised classification can be conducted using machine learning and non-machine learning algorithms. SVM is a type of supervised machine learning algorithm that works well in classification and regression. It uses a hyperplane (see Figure 5) to divide the support vectors to distinctly classify the data points, and there are many possible ways for the hyperplane to separate the support vectors in which, the main objective of SVM is to find the hyperplane that has the maximum margin (separate support vectors of both classes at a maximum distance) (Maxwell et al. 2018).

[Figure 5 near here]

SVM comprises of several hyperparameters: kernel type, gamma and penalty value. These hyperparameters can be tuned and adjusted to improve the performance of SVM in image classification.

3.3.2 Classification and Regression Tree

The CART is similar to DT. CART, which is a type of supervised machine learning algorithm that forms a binary decision tree. It involves the identification and construction of the tree using the training samples for which the correct classification is unknown. The decision tree starts with a root node derived from any variable in the feature space and minimises a measure of the impurity of the two sibling nodes (see Figure 6). Then, the decision tree grows by means of the successive subdivisions until it reaches a stage where

650
651
652 there is no significant reduction in the measure of impurity when further division is
653
654 implemented (Bittencourt and Clarke 2003; Jiang et al. 2010).
655
656
657
658
659

660 [Figure 6 near here]
661
662
663

664 The decision tree is made of multilevel and multi-leaf nodes and the decision tree will
665
666 undergo a pruning process once it is constructed. The constructed trees are often over-fit
667
668 because an excessive number of nodes and branches are often being created. Therefore, the
669
670 tree can be pruned by controlling the parameters or thresholds for the new branches (Calbury
671
672 2016).
673
674

675 676 3.3.3 Random Forest 677

678 RF or Random Decision Forest is a non-parametric machine learning algorithm that can be
679
680 used in both classification and regression analysis. It is a type of ensemble learning algorithm
681
682 that ensembles a number of decision trees and forms a forest (see Figure 7). This algorithm
683
684 combines random features or a combination of features at each node to grow a tree. The
685
686 bagging method is used in this algorithm to generate the training samples, and each selected
687
688 feature is drawn randomly by the replacement of N (size of original training set) examples.
689
690 The examples are classified based on the highest voted class produced from all the trees in
691
692 the forest (Pal 2005).
693
694
695
696
697
698

699 [Figure 7 near here]
700
701
702
703
704
705
706
707
708

One of the most frequently used attributes in the decision tree induction is the Gini Index. For a given training set T , selecting one case (pixel) at random and assuming that it belongs to some class C_i , the expression can be written as:

$$\sum_{j \neq i} (f(C_i, T)/|T|)((f(C_j, T)/|T|) \quad (1)$$

where $f(C_i, T)/|T|$ is the probability that the selected case belongs to class C_i . Gini Index acts as an attribute selection measure in RF that measures the impurity of an attribute with respect to the classes. Since RF works by assembling a number of trees, whereby N is to form a forest, the value of N can be defined by the user to get the best output of the classification. The RF algorithm can use a large number of trees in the ensemble and as a result, it works well in high dimensional data (Gislason et al. 2006).

3.3.4 Hyperparameters optimisation

Every algorithm has its own built-in hyperparameters/parameters that can be adjusted and further tuned to improve its performance. A hyperparameter is a parameter which contains a value that is set or defined before performing any learning process, and different model training algorithms consist of different hyperparameters. In this study, the hyperparameters in SVM, CART and RF algorithms were optimised in GEE, and the involved hyperparameters were tabulated in Table 3.

[Table 3 near here]

These hyperparameters are tuneable and can directly affect the robustness of the learning models, thus optimisation of the hyperparameters is required to achieve the best performance level of the algorithms. The identification of the hyperplane in SVM can be due to the type of kernel, k : Linear, Radial basis function, Polynomial and Sigmoid. Kernels are used to solve a

768
769
770 non-linear problem in a higher dimension and is usually referred to as kernel trick (Afonja
771 2017). Gamma, g is the hyperparameter in SVM that defines how far the influence of a
772 single training example reaches. A high value of gamma considers only nearby points (near
773 identified hyperplane) in the calculation. Conversely, low gamma considers far away points
774 to be included in the calculation for the separation of the hyperplane (Patel 2017). As for the
775 penalty or regularisation hyperparameter, C in SVM is to avoid misclassification in the
776 learning model. A larger value of C tells SVM to produce a smaller-margin hyperplane and
777 on the contrary, a small value of C enlarges the margin of the hyperplane.
778
779
780
781
782
783
784
785
786
787
788
789
790
791

[Figure 8 near here]

792
793 In this study, a total of four hyperparameters were fine-tuned in CART. Firstly, the cross-
794 validation factor, cv in CART partitions of the training samples were tuned into K (number of
795 folds) equally sized subsamples. Assuming that the training samples were divided into 10
796 folds of subsamples, 9 of the subsamples are used as training data and the other 1 subsample
797 as validation as shown in Figure 8 (Ivanovic 2016). Then, max depth, d is used to determine
798 the maximum of the tree depth in the model. The number of terminal nodes increases
799 proportionally to the depth of the tree. For d equals to 1 will have 2 terminal nodes, and d
800 equals to 2 will have a maximum of 4 nodes. The maximum of the nodes in a tree depends on
801 the depth of the tree by implementing the rule of 2 to the power of d (Molnar 2016).
802
803
804
805
806
807
808
809
810
811
812
813
814
815
816
817
818
819
820
821
822
823
824
825
826

3.4 McNemar's test

McNemar's test is a statistical test that applies to 2 x 2 contingency table. Sometimes, it is known as McNemar's Chi-Square test because it has a chi-square distribution. McNemar's test is conducted to determine whether if there are differences on a dichotomous dependent variable between two related classifiers or groups (Pal et al. 2013). The McNemar's test has been used by Yu et al. (2017) to determine the difference between classifications based on other pairs of features. Duro et al. (2012) performed McNemar's test to compare the classification results between DT, RF and SVM via object-based and pixel-based techniques. The result showed that the p-value via object-based was statistically significant ($p < 0.05$) when comparing DT with either RF or SVM. On the other hand, no statistically significant difference ($p > 0.05$) was produced when comparing the results obtained from different algorithms via pixel-based technique.

4. Results and Discussion

4.1 Land cover classifications

This study was aimed to produce an oil palm land cover map over Peninsular Malaysia by comparing SVM, CART and RF machine learning algorithms in the GEE platform. A total of 7 classes (water, built-up, bare soil, forest, oil palm, other vegetation and paddy) were classified. However, the classification output analysis emphasized only on oil palm because the produced oil palm map will later be used to evaluate the spatial distribution of oil palm in Peninsular Malaysia and will be included into a Geographic Information System (GIS) database for further analysis. The hyperparameters were optimised and classified maps produced by the algorithms are shown in Figure 9.

886
887
888 [Figure 9 near here]
889
890
891
892

893 The hyperparameters optimisation was carried out in the GEE. A grid search method was
894 implemented for each algorithm to find the best hyperparameters to be used for the
895 classification (Gupta et al. 2018). Generally, the hyperparameters used to produce the outputs
896 for each algorithm are as shown in Table 3.
897
898

899
900
901
902 In this study, 7 classes were identified in which, water classified features with water elements
903 such as lakes, sea, rivers and ponds. Built-up classified buildings, metals, concretes and
904 roads. Then, bare soil classified features that are bare land, open areas and places full of sand
905 or soil (such as construction site). Oil palm classified oil palm trees while other vegetation
906 classified features other than oil palm and forests such as shrubs, other crops and plantations.
907
908 Since the aim of this study was to test the performance of machine learning algorithms to
909 extract oil palm plantation from 30 m Landsat 8 images in the cloud-based, GEE platform,
910 additional information such as NDVI, NDWI and slope were included to enhance the
911 classification, especially in distinguishing one class from another. The produced oil palm map
912 provides the information on the oil palm distribution for 2017 and furthermore, the map can
913 later be used in the future studies such as to evaluate the impact of oil palm land cover in
914 detailed.
915
916
917
918
919
920
921
922
923
924
925
926
927
928
929
930

931 **4.2 Overall accuracies and land cover maps comparison**

932

933 A total of 30% of testing samples (water: 213, built-up: 311, bare soil: 126, forest: 470, oil
934 palm: 331, other vegetation: 276 and paddy: 119) were used to validate the classified land
935 cover maps, and the overall accuracies obtained for each state were calculated (see Table 4).
936
937
938
939

940 The total area of oil palm in Peninsular Malaysia produced by CART, RF and SVM were
941
942
943
944

945
946
947 3005758 ha, 2795287 ha and 2924434 ha respectively. Table 4 indicates that SVM produced
948
949 the highest overall accuracy with an average of 93.16%. That is followed by the overall
950
951 accuracies produced by RF and CART with an average of 86.50% and 80.08% respectively.
952
953
954 The overall accuracies produced were calculated via confusion matrix based on the
955
956 accuracies of the 7 classified classes.
957
958
959
960
961
962
963
964
965
966
967
968
969
970
971
972
973
974
975
976
977
978
979
980
981
982
983
984
985
986
987
988
989
990
991
992
993
994
995
996
997
998
999
1000
1001
1002
1003

1004
1005
1006
1007
1008
1009
1010
1011
1012
1013
1014
1015
1016
1017
1018
1019
1020
1021
1022
1023
1024
1025
1026
1027
1028
1029
1030
1031
1032
1033
1034
1035
1036
1037
1038
1039
1040
1041
1042
1043
1044

[Table 4 near here]

1045
1046
1047
1048
1049
1050
1051
1052
1053
1054
1055
1056
1057
1058
1059
1060
1061
1062
1063
1064
1065
1066
1067
1068
1069
1070
1071
1072
1073
1074
1075
1076
1077
1078
1079
1080
1081
1082
1083
1084
1085

[Table 5 near here]

1086
1087
1088
1089 By referring to the inventory provided by the Malaysia Palm Oil Board (MPOB), the area of
1090
1091 oil palm plantations produced by SVM, CART and RF were compared for each state in
1092
1093 Peninsular Malaysia. Table 5 shows the difference of oil palm area produced by SVM, CART
1094
1095 and RF by comparing the generated results with the MPOB inventory. However, the
1096
1097 limitation of 30 m coarse resolution data, RF, CART and SVM have overestimated the oil
1098
1099 palm area and misclassified other classes as oil palm land cover. Based on the classified oil
1100
1101 palm areas tabulated in Table 5, most of the states overestimated the oil palm areas. Kedah
1102
1103 overestimated more than 60000 ha and followed by Selangor with an overestimation of more
1104
1105 than 56000 ha of oil palm area. Then, the result showed that at least 1000 ha of land area was
1106
1107 misclassified as oil palm in Perlis. This is because the misclassified pixels were due to the
1108
1109 similarity of the reflectance value of the pixels. Therefore, the pixels that were misclassified
1110
1111 as oil palms have contributed to the overestimation of the oil palm area for the
1112
1113 aforementioned states. Conversely, all three algorithms underestimated the oil palm area for
1114
1115 Melaka. Overall, all the machine learning algorithms, SVM, RF and CART overestimated the
1116
1117 oil palm area for Peninsular Malaysia. Although SVM produced the highest overall accuracy,
1118
1119 RF produced the least errors in comparison with the MPOB inventory in oil palm
1120
1121 classification by producing an overall error of 0.03%, followed by SVM and CART with
1122
1123 0.08% and 0.11% for the whole oil palm area of Peninsular Malaysia respectively.
1124
1125 Furthermore, RF classified oil palm land cover and produced the nearest result (oil palm area)
1126
1127 to the MPOB inventory for most of the states: Negeri Sembilan, Pulau Pinang, Kedah,
1128
1129 Pahang, Perak, Perlis and Terengganu. Then, CART extracted the most accurate oil palm
1130
1131 areas for Johor and Kelantan, and SVM extracted the best for Melaka.
1132
1133
1134
1135
1136
1137

1138 This study had tested the performance of three algorithms (CART, RF and SVM) with
1139
1140 fine-tuned hyperparameters on 30 m Landsat data, and managed to produce oil palm land
1141
1142
1143
1144

1145
1146
1147 cover maps over Peninsular Malaysia using a cloud-based platform, GEE. The powerful
1148 cloud computing platform, GEE has made mapping oil palm land cover over Peninsular
1149 Malaysia using Landsat data possible. However, this study has confronted a few setbacks.
1150 Firstly, the utilisation of 30 m spatial resolution data might produce errors due to mixed
1151 pixels and furthermore, there might be more than one class in a single pixel. Then, the
1152 similarity of the reflectance between other vegetation and oil palm as well as between bare
1153 soil and built-up had caused confusion in the classification. Furthermore, the images used
1154 were the result from image patching, in which the product might contain errors in the pixels,
1155 hence reducing the quality of the image. Peninsular Malaysia is a huge area, and to obtain a
1156 single cloud-free image for a tropical region covering such huge area is merely impossible.
1157 Thus, image patching is one of the alternatives to obtain an almost cloud-free data. Therefore,
1158 it is challenging to ensure the quality of optical data, especially when it involves huge tropical
1159 area.
1160
1161
1162
1163
1164
1165
1166
1167
1168
1169
1170
1171
1172
1173
1174
1175
1176
1177
1178
1179
1180

1181 [Figure 10 near here]
1182
1183
1184
1185
1186
1187
1188
1189
1190
1191
1192
1193
1194
1195
1196
1197
1198
1199
1200
1201
1202
1203

1204
1205
1206
1207
1208
1209
1210
1211
1212
1213
1214
1215
1216
1217
1218
1219
1220
1221
1222
1223
1224
1225
1226
1227
1228
1229
1230
1231
1232
1233
1234
1235
1236
1237
1238
1239
1240
1241
1242
1243
1244

[Figure 11 near here]

1245
1246
1247
1248
1249
1250
1251
1252
1253
1254
1255
1256
1257
1258
1259
1260
1261
1262
1263
1264
1265
1266
1267
1268
1269
1270
1271
1272
1273
1274
1275
1276
1277
1278
1279
1280
1281
1282
1283
1284
1285
1286
1287
1288
1289
1290
1291
1292
1293
1294
1295
1296
1297
1298
1299
1300
1301
1302
1303

Figures 10 and 11 are the selected focused regions in Pulau Pinang and Selangor respectively that were classified by CART, RF and SVM. The feature (in the red box) showed in Figure 10(a) is oil palm trees. Based on the classified images (Figures 10(b), 10(c) and 10(d)), the result showed that SVM misclassified most of the oil palm pixels as other vegetation. Furthermore, SVM misinterpreted the bare soil pixels with built-up in Selangor as shown in Figure 11(d). On the other hand, the oil palm and bare soil pixels for both areas (Selangor and Pulau Pinang) were found to be well classified by CART and RF. These findings showed that the utilisation of additional layers (NDVI, NDWI and others) in the tree methods implemented in RF and CART is more efficient. In addition, both tree-based algorithms (RF and CART) can classify the pixels better than the SVM that works via maximizing the hyperplane. Moreover, the failure of SVM algorithm in separating the support vectors had led to classification errors. As for RF and CART, the RF algorithm has improved the classification as the trees in the RF were ensembled into a forest, and finally the classes were defined based on the majority vote. Although Figures 10 and 11 showed that SVM misclassified oil palm and bare soil pixels, the best algorithm to classify all the 7 classes for the whole Peninsular Malaysia is SVM. However, by comparing all three machine learning algorithms, this study agreed that RF extracted oil palm class the best for the whole Peninsular Malaysia.

4.3 McNemar's test

McNemar's test has been carried out in this study to measure the significance between the classification of SVM and CART, SVM and RF and CART and RF. The 2 x 2 contingency table as tabulated in Table 6 was used to calculate the p-values.

[Table 6 near here]

The null hypothesis of this test states that the probability of Test 1 being correctly classified is equal to the probability of Test 2 being correctly classified. Also, the probability of Test 1 being incorrectly classified is equal to the probability of Test 2 being incorrectly classified. In other words, $P_a + P_b = P_a + P_c$ or $P_b + P_d = P_c + P_d$, which leads to $P_b = P_c$.

P_a = Probability of Test 1 being positive and Test 2 being positive
 P_b = Probability of Test 1 being positive and Test 2 being negative
 P_c = Probability of Test 1 being negative and Test 2 being positive
 P_d = Probability of Test 1 being negative and Test 2 being negative

The p-value will be calculated and the value of $p < 0.05$ is considered as a significant result, thus rejecting the null hypothesis. In this study, calculations of the p-value using the formula demonstrated by Foody (2004) were conducted for all the algorithms and the results are tabulated in Table 8.

[Table 7 near here]

The p-value obtained when comparing between SVM and RF is 0.28 ($p > 0.05$), while the other two comparisons obtained values of $p < 0.05$. Due to the robustness and powerful machine learning algorithms, SVM and RF algorithms can classify the pixels well. Hence, the comparison between SVM and RF gave a non-significant p-value > 0.05 and thus, accepted the null hypothesis.

5. Conclusion

In this study, we utilised 30 m Landsat data in the GEE platform to produce oil palm land cover maps over Peninsular Malaysia. The GEE platform is controllable and it provides

1363
1364
1365 options especially in selecting the processing methods, algorithms and data input.
1366
1367 Furthermore, it allows users to design the workflow based on their needs. In this study, three
1368 machine learning algorithms were used and the hyperparameters were tuned. Accuracy
1369 assessments for the classified maps were conducted using high-resolution Google Earth
1370 images and the map provided by the DOA. The comparison of the classified oil palm areas
1371 with the inventory provided by MPOB has shown that there is a large uncertainty of oil palm
1372 land cover in Perlis, Kedah and Selangor. Overall, CART, SVM and RF were able to classify
1373 the land cover maps and produced acceptable results by producing an overall accuracy of
1374 80.08%, 93.16% and 86.50% respectively. Then, McNemar's test was conducted and it
1375 showed that significant p-values were obtained when comparing CART to both SVM and RF.
1376 However, the test showed a non-significant value when comparing between RF and SVM.
1377 This shows that both methods can reliably be used to produce high accuracy maps in GEE
1378 and later be used to classify other crops. Moving on, such timely and high accuracy estimates
1379 of oil palm areas could be embedded with other ancillary GIS data for a variety of monitoring
1380 and decision-making applications, including yield prediction, supply-chain logistics,
1381 commodity markets, bioenergy estimation and more.

1382
1383
1384
1385
1386
1387
1388
1389
1390
1391
1392
1393
1394
1395
1396
1397
1398
1399
1400
1401
1402 GEE provides various geospatial data including Sentinel 2, Sentinel 1 and MODIS.
1403
1404 The utilisation of higher spatial resolution data such as Sentinel 2 with 20 m to 10 m of pixel
1405 size can be tested to improve the classification. Moreover, Sentinel 1 works with active
1406 sensors, and it is suitable to be used on tropical regions. The integration of Sentinel 1 data in
1407 the GEE platform can reduce the time needed to process huge amounts of radar data. On top
1408 of that, there are many more methods available in GEE to pre-process remote sensing data, in
1409 which some methods might produce good results and able to improve the accuracy of the
1410
1411
1412
1413
1414
1415
1416
1417
1418
1419
1420
1421

1422
1423
1424 data. In addition, the programmable platform produces the possibilities for the cloud
1425
1426 computing GEE to be integrated with the powerful deep learning methods.
1427
1428
1429
1430

1431 **Acknowledgements**

1432
1433 We would like to thank Universiti Putra Malaysia for their facilities and support for this research.
1434 Sponsorship from the Engineering and Physical Sciences Research Council UK (EPSRC/RCUK)
1435 (Grant Number: EP/P018165/1- Newton Fund) is gratefully acknowledged. The comments from the
1436 anonymous reviewers in improving this article are highly appreciated.
1437
1438
1439
1440

1441 **References**

1442
1443 Afonja T. 2017. Kernel functions. [accessed 2019 March 12].
1444
1445 <https://towardsdatascience.com/kernel-function-6f1d2be6091>.
1446
1447

1448
1449
1450 Belgiu M, Drăguț L. 2016. Random forest in remote sensing: A review of applications and
1451 future directions. ISPRS J Photogramm Remote Sens. 114:24-31.
1452 doi:10.1016/j.isprsjprs.2016.01.011.
1453
1454
1455

1456
1457 Bittencourt H, Clarke RT. 2003. Use of classification and regression trees (CART) to classify
1458 remotely-sensed digital images. In: IGARSS 2003. Proceedings of the IEEE Trans
1459 Geosci Remote Sens Symposium 2003. Toulouse, France, July 21–25: IEEE IGARSS.
1460 p. 3751–3753.
1461
1462
1463
1464

1465
1466 Brid RS. 2018. Decision trees. Medium; [accessed 2019 January 20].
1467
1468 [https://medium.com/greyatom/decision-trees-a-simple-way-to-visualize-a-decision-](https://medium.com/greyatom/decision-trees-a-simple-way-to-visualize-a-decision-dc506a403aeb)
1469 [dc506a403aeb](https://medium.com/greyatom/decision-trees-a-simple-way-to-visualize-a-decision-dc506a403aeb).
1470
1471

1472
1473 Bro-Jørgensen J, Brown ME, Pettorelli N. 2008. Using the satellite-derived normalized
1474 difference vegetation index (NDVI) to explain ranging patterns in a lek-breeding
1475
1476
1477
1478
1479
1480

1481
1482
1483 antelope: the importance of scale. *Oecologia*. 158(1):177-182. doi:10.1007/s00442-008-
1484 1121-z
1485
1486
1487

1488 Calbury. 2016. Object-based Classification: Classification and Regression Tree (CART).
1489 [Accessed 2019 March 3]. [wiki.landscapetoolbox.org/doku.php/remote_sensing_](http://wiki.landscapetoolbox.org/doku.php/remote_sensing_methods:classification_and_regression_tree_cart)
1490 [methods:classification_and_regression_tree_cart](http://wiki.landscapetoolbox.org/doku.php/remote_sensing_methods:classification_and_regression_tree_cart).
1491
1492
1493
1494

1495 Camacho A, Correa CV, Arguello H. 2019. An analysis of spectral variability in hyperspectral
1496 imagery: a case study of stressed oil palm detection in Colombia. *Int J Remote Sens*.
1497 40(19):7603-7623. doi:10.1080/01431161.2019.1595210.
1498
1499
1500
1501

1502 Chander G, Markham BL, Helder DL. 2009. Summary of current radiometric calibration
1503 coefficients for Landsat MSS, TM, ETM+, and EO-1 ALI sensors. *Remote Sens*
1504 *Environ*. 113(5):893-903. doi:10.1016/j.rse.2009.01.007.
1505
1506
1507
1508

1509 Charters LJ, Aplin P, Marston CG, Padfield R, Rengasamy N, Bin Dahalan MP, Evers S. 2019.
1510 Peat swamp forest conservation withstands pervasive land conversion to oil palm
1511 plantation in North Selangor, Malaysia. *Int J Remote Sens*.40(19):1-30.
1512 doi:10.1080/01431161.2019.1574996.
1513
1514
1515
1516
1517

1518 Cheng Y, Yu L, Cracknell AP, Gong P. 2016. Oil palm mapping using Landsat and PALSAR:
1519 A case study in Malaysia. *Int J Remote Sens*. 37(22):5431-5442.
1520 doi:10.1080/01431161.2016.1241448.
1521
1522
1523
1524

1525 Cheng Y, Yu L, Xu Y, Lu H, Cracknell AP, Kanniah K, Gong P. 2018. Mapping oil palm
1526 extent in Malaysia using ALOS-2 PALSAR-2 data. *Int J Remote Sens*. 39(2):432-452.
1527 doi:10.1080/01431161.2017.1387309.
1528
1529
1530
1531
1532
1533
1534
1535
1536
1537
1538
1539

1540
1541
1542 Chong KL, Kanniah KD, Pohl C, Tan KP. 2017. A review of remote sensing applications for
1543 oil palm studies. *Geo-spatial Information Science*. 20(2):184-200.
1544
1545 doi:10.1080/10095020.2017.1337317.
1546
1547
1548

1549 **De Alban, J, Connette G, Oswald P, Webb E. (2018). Combined Landsat and L-band SAR data**
1550 **improves land cover classification and change detection in dynamic tropical**
1551 **landscapes. *Remote Sensing*. 10(2):306. doi:10.3390/rs10020306.**
1552
1553
1554
1555

1556 Dong J, Xiao X, Menarguez MA, Zhang G, Qin Y, Thau D, Biradar C, Moore B. 2016.
1557 Mapping paddy rice planting area in northeastern Asia with Landsat 8 images,
1558 phenology-based algorithm and Google Earth Engine. *Remote Sens Environ*. 185:142-
1559 154. doi:10.1016/j.rse.2016.02.016.
1560
1561
1562
1563
1564

1565 Duro DC, Franklin SE, Dubé, MG. 2012. A comparison of pixel-based and object-based image
1566 analysis with selected machine learning algorithms for the classification of agricultural
1567 landscapes using SPOT-5 HRG imagery. *Remote Sens Environ*. 118:259-272.
1568
1569 doi:10.1016/j.rse.2011.11.020.
1570
1571
1572
1573

1574 Fahmi Z, Samah BA, Abdullah H. 2013. Paddy industry and paddy farmers well-being: a
1575 success recipe for agriculture industry in Malaysia. *Asian Soc Sci*. 9(3):177-181.
1576
1577 doi:10.5539/ass.v9n3p177.
1578
1579
1580

1581 Fawcett D, Azlan B, Hill TC, Kho LK, Bennie J, Anderson K. 2019. Unmanned aerial vehicle
1582 (UAV) derived structure-from-motion photogrammetry point clouds for oil palm (*Elaeis*
1583 *guineensis*) canopy segmentation and height estimation. *Int J Remote Sens*. 40(19):1-23.
1584
1585 doi:10.1080/01431161.2019.1591651.
1586
1587
1588
1589

1590 Fitzherbert EB, Struebig MJ, Morel A, Danielsen F, Brühl CA, Donald PF, Phalan B. 2008.
1591 How will oil palm expansion affect biodiversity?. *Trends Ecol Evol*. 23(10):538-545.
1592
1593 doi:10.1016/j.tree.2008.06.012.
1594
1595
1596
1597
1598

- 1599
1600
1601 Gambo J, Shafri HZM, Shaharum NSN, Abidin FAZ, Rahman MTA. 2018. Monitoring and
1602 Predicting Land Use-Land Cover (LULC) Changes Within and Around Krau Wildlife
1603 Reserve (KWR) Protected Area in Malaysia Using Multi-Temporal Landsat Data.
1604 Geoplanning: journal of geomatics and planning. 5(1):23-44.
1605 doi:10.14710/geoplanning.5.1.17-34.
1606
1607
1608
1609
1610
1611
1612 Gislason PO, Benediktsson JA, Sveinsson JR. 2006. Random forests for land cover
1613 classification. Pattern Recognit Lett. 27(4):294-300. doi:10.1016/j.patrec.2005.08.011.
1614
1615
1616
1617
1618 Glinskis EA, Gutiérrez-Vélez VH. 2019. Quantifying and understanding land cover changes
1619 by large and small oil palm expansion regimes in the Peruvian Amazon. Land Use
1620 Policy. 80:95-106. doi:10.1016/j.landusepol.2018.09.032.
1621
1622
1623
1624
1625 Goldblatt R, You W, Hanson G, Khandelwal A. 2016. Detecting the boundaries of urban areas
1626 in india: A dataset for pixel-based image classification in google earth engine. Remote
1627 sensing. 8(8):634. doi:10.3390/rs8080634.
1628
1629
1630
1631
1632 Gorelick N, Hancher M, Dixon M, Ilyushchenko S, Thau D, Moore R. 2017. Google Earth
1633 Engine: Planetary-scale geospatial analysis for everyone. Remote Sens Environ. 202:18-
1634 27. doi:/10.1016/j.rse.2017.06.031.
1635
1636
1637
1638
1639 Gutiérrez-Vélez VH, DeFries R. 2013. Annual multi-resolution detection of land cover
1640 conversion to oil palm in the Peruvian Amazon. Remote Sens Environ. 129:154-167.
1641 doi:10.1016/j.rse.2012.10.033.
1642
1643
1644
1645
1646 Gupta O, Das AJ, Hellerstein J, Raskar R. 2018. Machine learning approaches for large scale
1647 classification of produce. Sci Rep. 8(1):5226-5233.
1648
1649
1650
1651
1652
1653
1654
1655
1656
1657

1658
1659
1660 Ivanovic B. 2016. Cross-validation and decision trees. [accessed 2019 January 15].
1661
1662 https://www.cs.utoronto.ca/~fidler/teaching/2015/slides/CSC411/tutorial3_CrossVal-
1663 [DTs.pdf](https://www.cs.utoronto.ca/~fidler/teaching/2015/slides/CSC411/tutorial3_CrossVal-DTs.pdf).
1664
1665
1666

1667 Jiang L, Wang W, Yang X, Xie N, Cheng Y. 2010. Classification methods of remote sensing
1668 image based on decision tree technologies. Paper presented at CCTA 2010. International
1669 Conference on Computer and Computing Technologies in Agriculture; Oct 20–25;
1670 Nanchang, China.
1671
1672
1673
1674
1675

1676 Joshi N, Baumann M, Ehammer A, Fensholt R, Grogan K, Hostert P, Jepsen MR, Kuemmerie
1677 T, Meyfroidt P, Mitchard ETA, Reiche J, Ryan CM, Waske B. (2016). A review of the
1678 application of optical and radar remote sensing data fusion to land use mapping and
1679 monitoring. *Remote Sensing*. 8(1):70. doi:10.3390/rs8010070.
1680
1681
1682
1683
1684

1685 Jusoff K, Pathan M. 2009. Mapping of individual oil palm trees using airborne hyperspectral
1686 sensing: an overview. *Applied physics research*. 1(1):15-30.
1687
1688

1689 Lee JSH, Wich S, Widayati A, Koh LP. 2016. Detecting industrial oil palm plantations on
1690 Landsat images with Google Earth Engine. *Remote sensing applications: society and*
1691 *environment*. 4:219-224. doi:10.1016/j.rsase.2016.11.003.
1692
1693
1694
1695
1696

1697 Li L, Dong J, Tengku SN, Xiao X. 2015. Mapping oil palm plantations in Cameroon using
1698 PALSAR 50-m orthorectified mosaic images. *Remote sensing*. 7(2):1206-1224.
1699 doi:10.3390/rs70201206.
1700
1701
1702
1703

1704 Li W, Fu H, Yu L, Cracknell A. (2016). Deep learning based oil palm tree detection and
1705 counting for high-resolution remote sensing images. *Remote Sensing*. 9(1):22.
1706 doi:https://doi.org/10.3390/rs9010022.
1707
1708
1709
1710
1711
1712
1713
1714
1715
1716

- 1717
1718
1719 Mahidin MU. 2018. Selected Agricultural Indicators Malaysia. Malaysia: Department
1720 of Statistics Malaysia; [accessed 2019 March 15].
1721
1722 [https://www.dosm.gov.my/v1/index.php?r=column/cthemByCat&cat=72&bul_id=Uj](https://www.dosm.gov.my/v1/index.php?r=column/cthemByCat&cat=72&bul_id=UjYxeDNkZ0xOUjhFeHpna20wUUJOUT09&menu_id=Z0VTZGU1UHBUT1VJMF1paXRRR0xpdz09)
1723 [YxeDNkZ0xOUjhFeHpna20wUUJOUT09&menu_id=Z0VTZGU1UHBUT1VJMF1pa](https://www.dosm.gov.my/v1/index.php?r=column/cthemByCat&cat=72&bul_id=UjYxeDNkZ0xOUjhFeHpna20wUUJOUT09&menu_id=Z0VTZGU1UHBUT1VJMF1paXRRR0xpdz09)
1724 [XRRR0xpdz09](https://www.dosm.gov.my/v1/index.php?r=column/cthemByCat&cat=72&bul_id=UjYxeDNkZ0xOUjhFeHpna20wUUJOUT09&menu_id=Z0VTZGU1UHBUT1VJMF1paXRRR0xpdz09).
1725
1726
1727
1728
1729
1730
1731 Maxwell AE, Warner TA, Fang F. 2018. Implementation of machine-learning classification in
1732 remote sensing: An applied review. *Int J Remote Sens.* 39(9):2784-2817.
1733 doi:10.1080/01431161.2018.1433343.
1734
1735
1736
1737
1738 Miettinen J, Shi C, Tan WJ, Liew SC. 2012. 2010 land cover map of insular Southeast Asia in
1739 250-m spatial resolution. *Pattern Recognit Lett.* 3(1):11-20.
1740 doi:10.1080/01431161.2010.526971.
1741
1742
1743
1744
1745 Molnar C. 2016. Interpretable Machine Learning: A Guide for Making Black Box Models
1746 Explainable. 1st ed. Christoph Molnar. [accessed 2019 January 20].
1747 <https://christophm.github.io/interpretable-ml-book/tree.html>.
1748
1749
1750
1751
1752 Morel AC, Fisher JB, Malhi Y. 2012. Evaluating the potential to monitor aboveground biomass
1753 in forest and oil palm in Sabah, Malaysia, for 2000–2008 with Landsat ETM+ and ALOS-
1754 PALSAR. *Int J Remote Sens.* 33(11):3614-3639. doi:10.1080/01431161.2011.631949.
1755
1756
1757
1758
1759 Nambiappan B, Ismail A, Hashim N, Ismail N, Shahari DN, Idris NAN, Omar N, Salleh KM,
1760 Hassan NAM, Din AK. 2018. Malaysia: 100 years of resilient palm oil economic
1761 performance. *J. Oil Palm Res.* 30(1):13-25. doi:10.21894/jopr.2018.0014.
1762
1763
1764
1765
1766 Ng WPQ, Lam HL, Ng FY, Kamal M, Lim JHE. 2012. Waste-to-wealth: green potential from
1767 palm biomass in Malaysia. *J Clean Prod.* 34:57-65. doi:10.1016/j.jclepro.2012.04.004.
1768
1769
1770
1771
1772
1773
1774
1775

- 1776
1777
1778
1779
1780
1781
1782
1783
1784
1785
1786
1787
1788
1789
1790
1791
1792
1793
1794
1795
1796
1797
1798
1799
1800
1801
1802
1803
1804
1805
1806
1807
1808
1809
1810
1811
1812
1813
1814
1815
1816
1817
1818
1819
1820
1821
1822
1823
1824
1825
1826
1827
1828
1829
1830
1831
1832
1833
1834
- Noi PT, Kappas M. 2018. Comparison of random forest, k-nearest neighbor, and support vector machine classifiers for land cover classification using Sentinel-2 imagery. *Sensors*. 18(1):1-20. doi:10.3390/s18010018.
- Nooni IK, Duker AA, Van Duren I, Addae-Wireko L, Osei Jnr EM. 2014. Support vector machine to map oil palm in a heterogeneous environment. *Int J Remote Sens*. 35(13):4778-4794. doi:10.1080/01431161.2014.930201.
- Oliphant AJ, Thenkabail PS, Teluguntla P, Xiong J, Gumma MK, Congalton RG, Yadav K. 2019. Mapping cropland extent of Southeast and Northeast Asia using multi-year time-series Landsat 30-m data using a random forest classifier on the Google Earth Engine Cloud. *Int J Appl Earth Obs Geoinf*. 81:110-124. doi:10.1016/j.jag.2018.11.014.
- Pal M. 2005. Random forest classifier for remote sensing classification. *Int J Remote Sens*. 26(1):217-222. doi:10.1080/01431160412331269698.
- Pal M, Maxwell AE, Warner TA. 2013. Kernel-based extreme learning machine for remote-sensing image classification. *Pattern Recognit Lett*. 4(9):853-862. doi:10.1080/2150704X.2013.805279.
- Patel NN, Angiuli E, Gamba P, Gaughan A, Lisini G, Stevens FR, Tatem AJ, Trianni G. 2015. Multitemporal settlement and population mapping from Landsat using Google Earth Engine. *Int J Appl Earth Obs Geoinf*. 35:199-208. doi:10.1016/j.jag.2014.09.005.
- Patel S. 2017. Chapter 2: SVM (Support Vector Machine) — Theory. [accessed 2019 March 10]. <https://medium.com/machine-learning-101/chapter-2-svm-support-vector-machine-theory-f0812effc72>.
- Roy DP, Wulder MA, Loveland TR, Woodcock CE, Allen RG, Anderson MC, Helder D, Irons JR, Johnson DM, Kennedy R, et al. 2014. Landsat-8: Science and product vision for

1835
1836
1837 terrestrial global change research. *Remote Sens Environ.* 145:154-172.
1838
1839 doi:10.1016/j.rse.2014.02.001.
1840
1841

1842 Shafri HZM, Hamdan N. 2009. Hyperspectral imagery for mapping disease infection in oil
1843 palm plantation using vegetation indices and red edge techniques. *Am J Appl Sci.*
1844
1845 6(6):1031-1035.
1846
1847

1848
1849 Shafri HZM, Anuar MI, Seman IA, Noor NM. 2011. Spectral discrimination of healthy and
1850
1851 Ganoderma-infected oil palms from hyperspectral data. *Int J Remote Sens.* 32(22):7111-
1852
1853 7129. doi:10.1080/01431161.2010.519003.
1854
1855

1856 Shahar FM. 2016 March 18. Heat wave emergency if temperature exceeds 40 degrees Celsius
1857
1858 for more than 7 days. *New Straits Times.* [accessed 2019 January 20].
1859
1860 [https://www.nst.com.my/news/2016/03/133534/heat-wave-emergency-if-temperature-](https://www.nst.com.my/news/2016/03/133534/heat-wave-emergency-if-temperature-exceeds-40-degrees-celcius-more-7-days)
1861
1862 [exceeds-40-degrees-celcius-more-7-days.](https://www.nst.com.my/news/2016/03/133534/heat-wave-emergency-if-temperature-exceeds-40-degrees-celcius-more-7-days)
1863
1864

1865 Shaharum NSN, Shafri HZM, Gambo J, Abidin FAZ. 2018. Mapping of Krau Wildlife Reserve
1866
1867 (KWR) protected area using Landsat 8 and supervised classification
1868
1869 algorithms. *Remote Sensing Applications: Society and Environment.* 10:24-35.
1870
1871 doi:10.1016/j.rsase.2018.01.002.
1872
1873

1874 Shaharum NSN, Shafri HZM, Ghani WAWAK, Samsatli S, Prince HM, Yusuf B, Hamud AM.
1875
1876 2019. Mapping the spatial distribution and changes of oil palm land cover using an open
1877
1878 source cloud-based mapping platform. *Int J Remote Sens.* 40(19):1-18.
1879
1880 doi:10.1080/01431161.2019.1597311.
1881
1882

1883 Shelestov A, Lavreniuk M, Kussul N, Novikov A, Skakun S. 2017. Exploring Google earth
1884
1885 engine platform for Big Data Processing: Classification of multi-temporal satellite
1886
1887 imagery for crop mapping. *Front Earth Sci.* 5(17):1-10. doi:10.3389/feart.2017.00017.
1888
1889
1890
1891
1892
1893

- 1894
1895
1896 Shuit SH, Tan KT, Lee KT, Kamaruddin AH. 2009. Oil palm biomass as a
1897 sustainable energy source: A Malaysian case study. *Energy*. 34(9):1225-1235.
1898 doi:10.1016/j.energy.2009.05.008.
1899
1900
1901
1902
1903 Sidhu N, Pebesma E, Câmara G. 2018. Using Google Earth Engine to detect land
1904 cover change: Singapore as a use case. *Eur J Remote Sens*. 51(1):486-500.
1905 doi:10.1080/22797254.2018.1451782.
1906
1907
1908
1909
1910 Thenkabail PS, Stucky N, Griscom BW, Ashton MS, Diels J, Van Der Meer B, Enclona E.
1911 2004. Biomass estimations and carbon stock calculations in the oil palm plantations of
1912 African derived savannas using IKONOS data. *Int J Remote Sens*. 25(23):5447-5472.
1913 doi:10.1080/01431160412331291279.
1914
1915
1916
1917
1918
1919 Yu X, Hyypä J, Litkey P, Kaartinen H, Vastaranta M, Holopainen M. 2017. Single-sensor
1920 solution to tree species classification using multispectral airborne laser scanning. *Remote*
1921 *Sensing*. 9(2):108-123. doi:10.3390/rs9020108.
1922
1923
1924
1925
1926
1927
1928
1929
1930
1931
1932
1933
1934
1935
1936
1937
1938
1939
1940
1941
1942
1943
1944
1945
1946
1947
1948
1949
1950
1951
1952

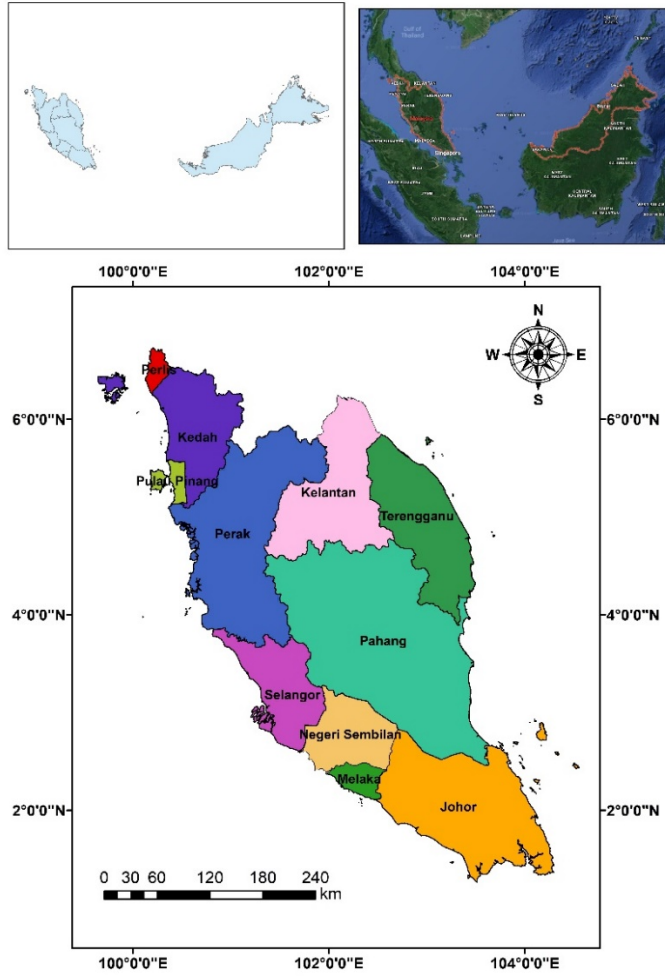


Figure 1. Location of the study area: Peninsular Malaysia.

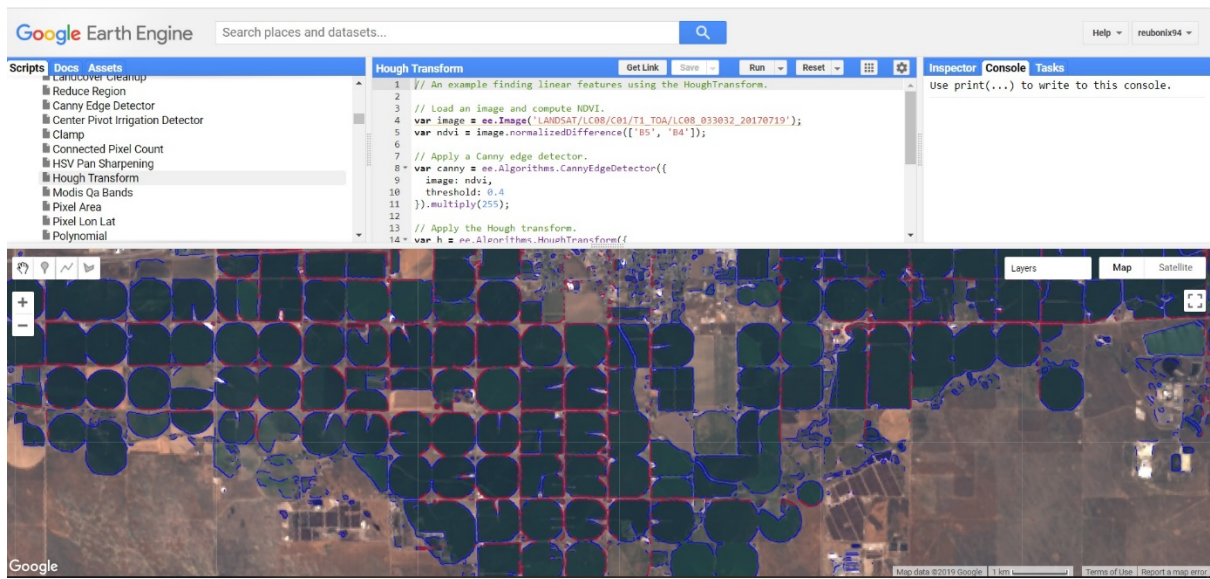


Figure 2. The Earth Engine Javascript API.

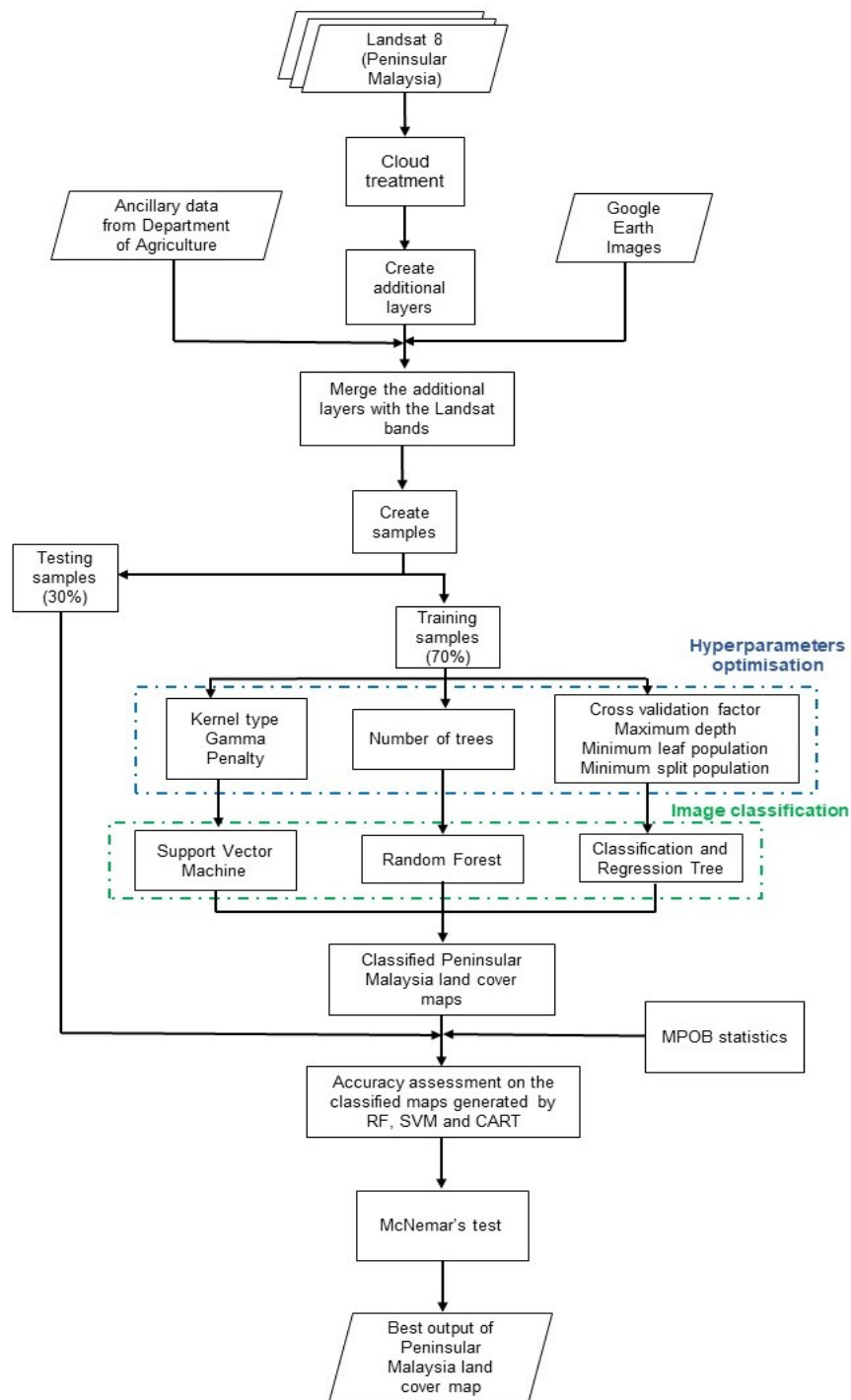


Figure 3. Methodological steps conducted for this study.

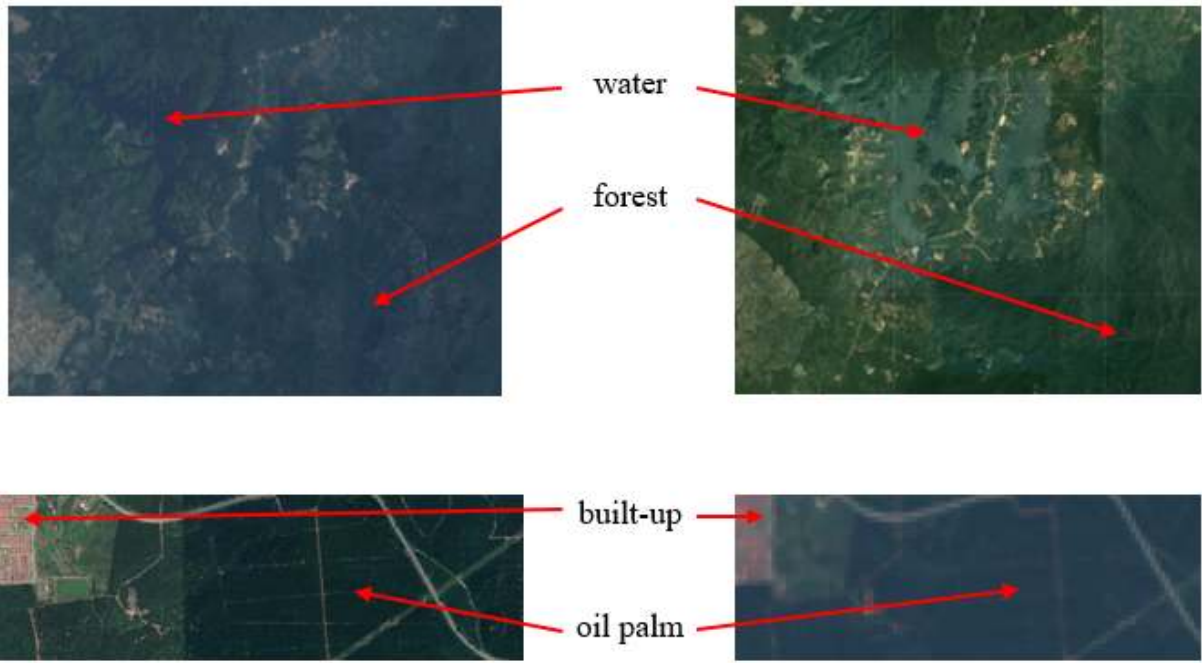


Figure 4. (a) High-resolution Google Earth image, (b) Landsat 8 image.

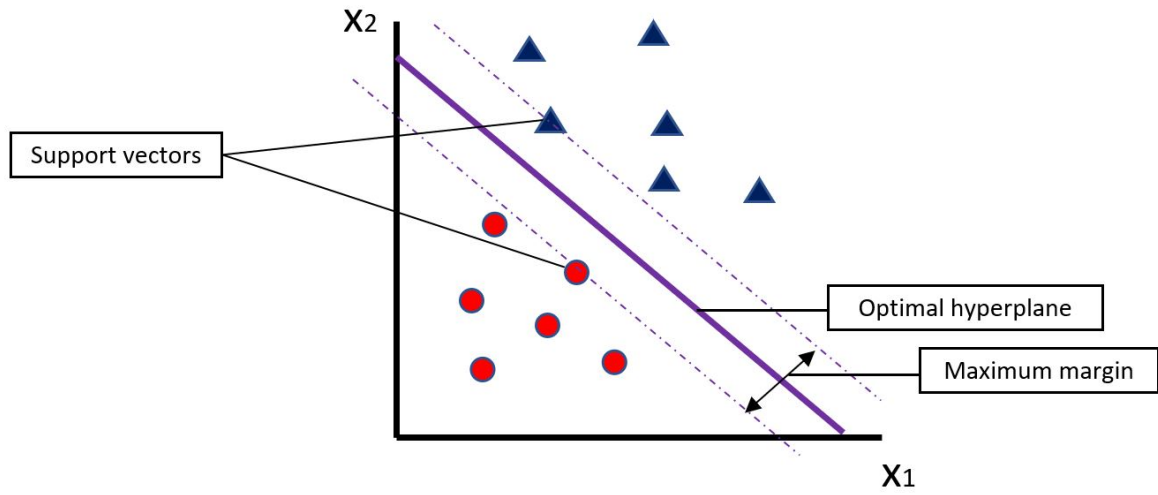


Figure 5. Optimal hyperplane identification in SVM.

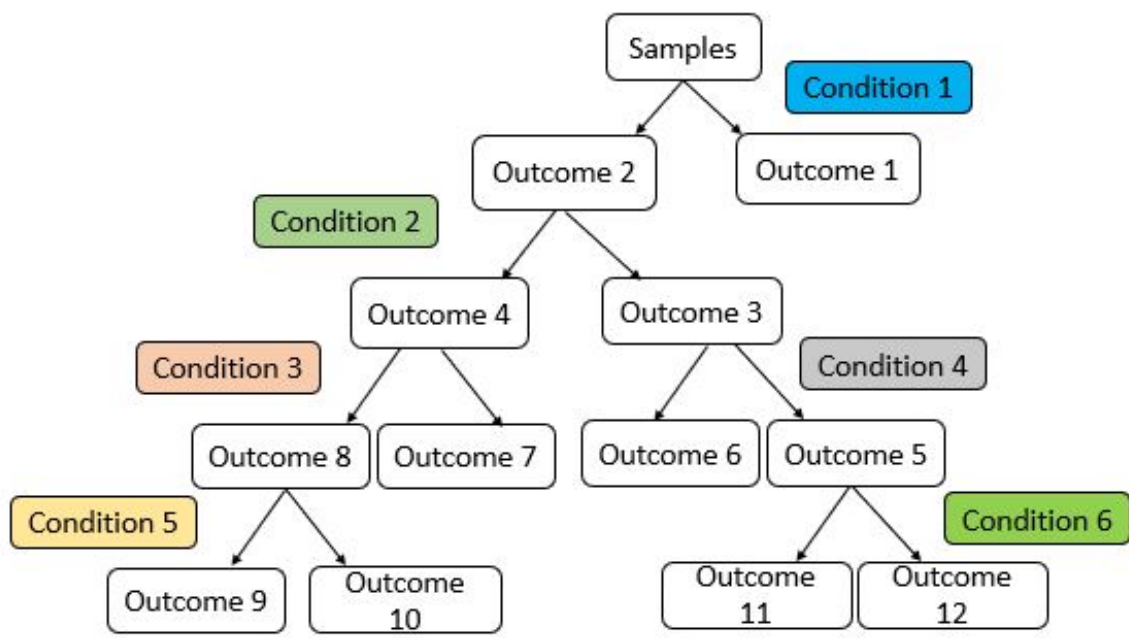


Figure 6. The division of the tree in CART.

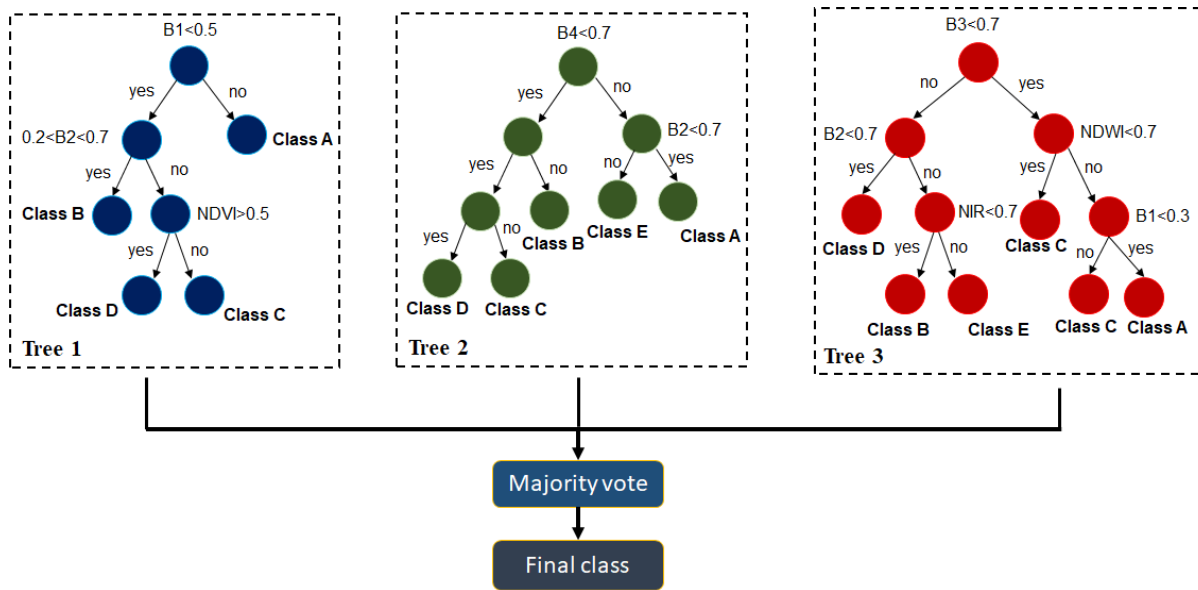


Figure 7. Example of trees ensemble in the RF structure.

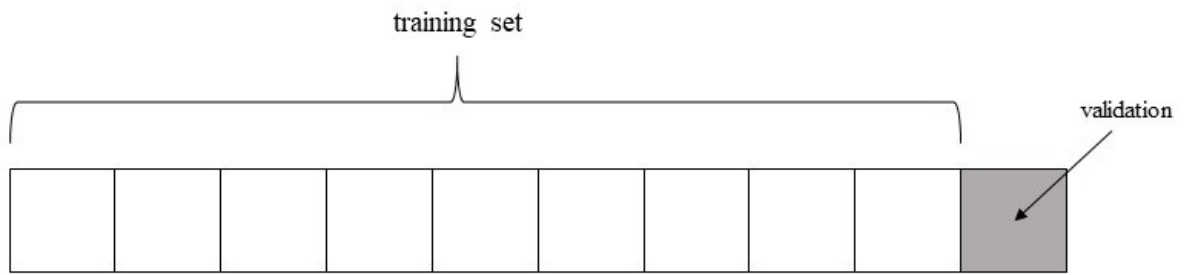


Figure 8. Subsamples in cross validation.

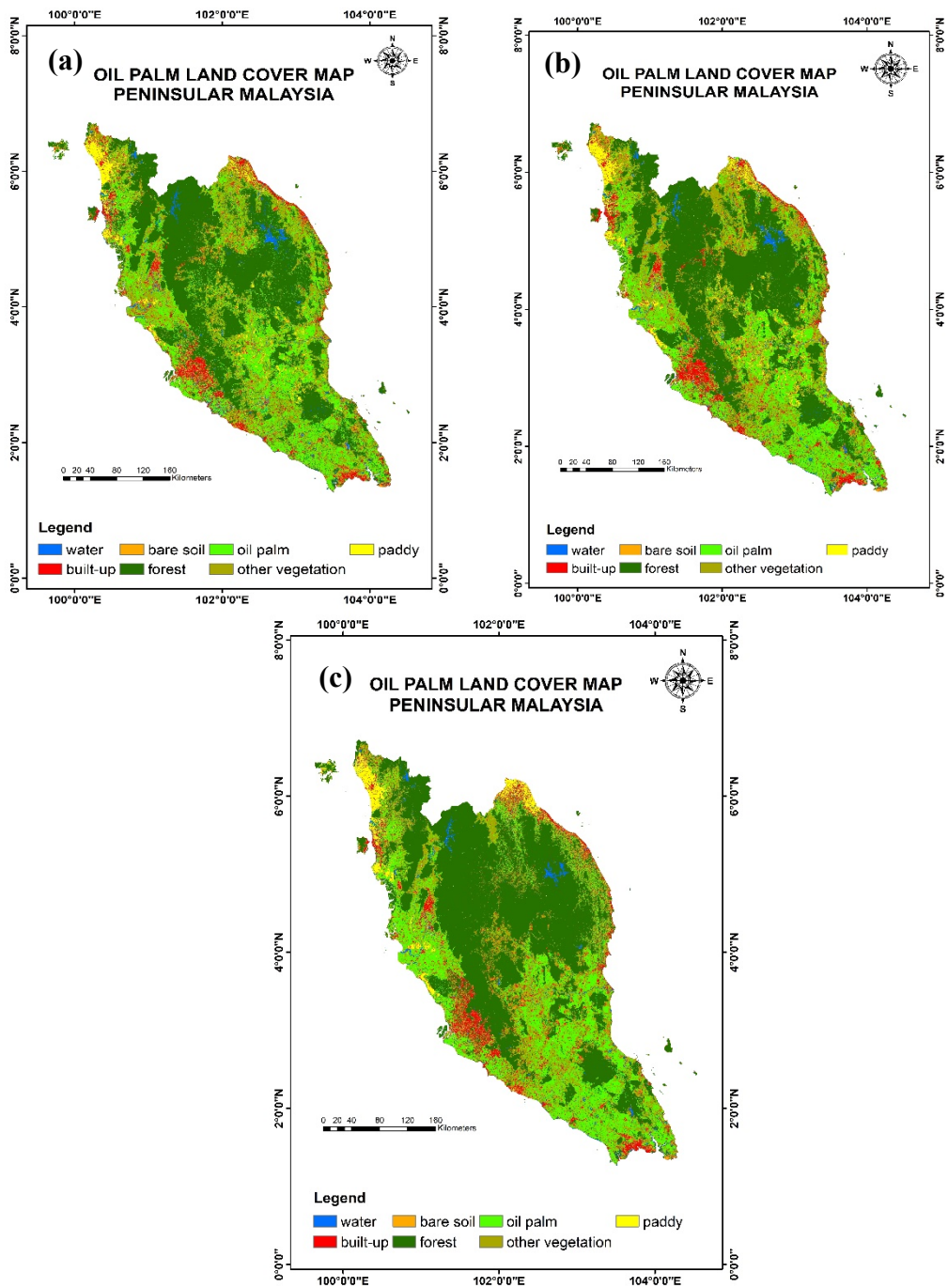


Figure 9. Classified oil palm land cover maps of Peninsular Malaysia, (a) CART, (b) RF and (c) SVM.

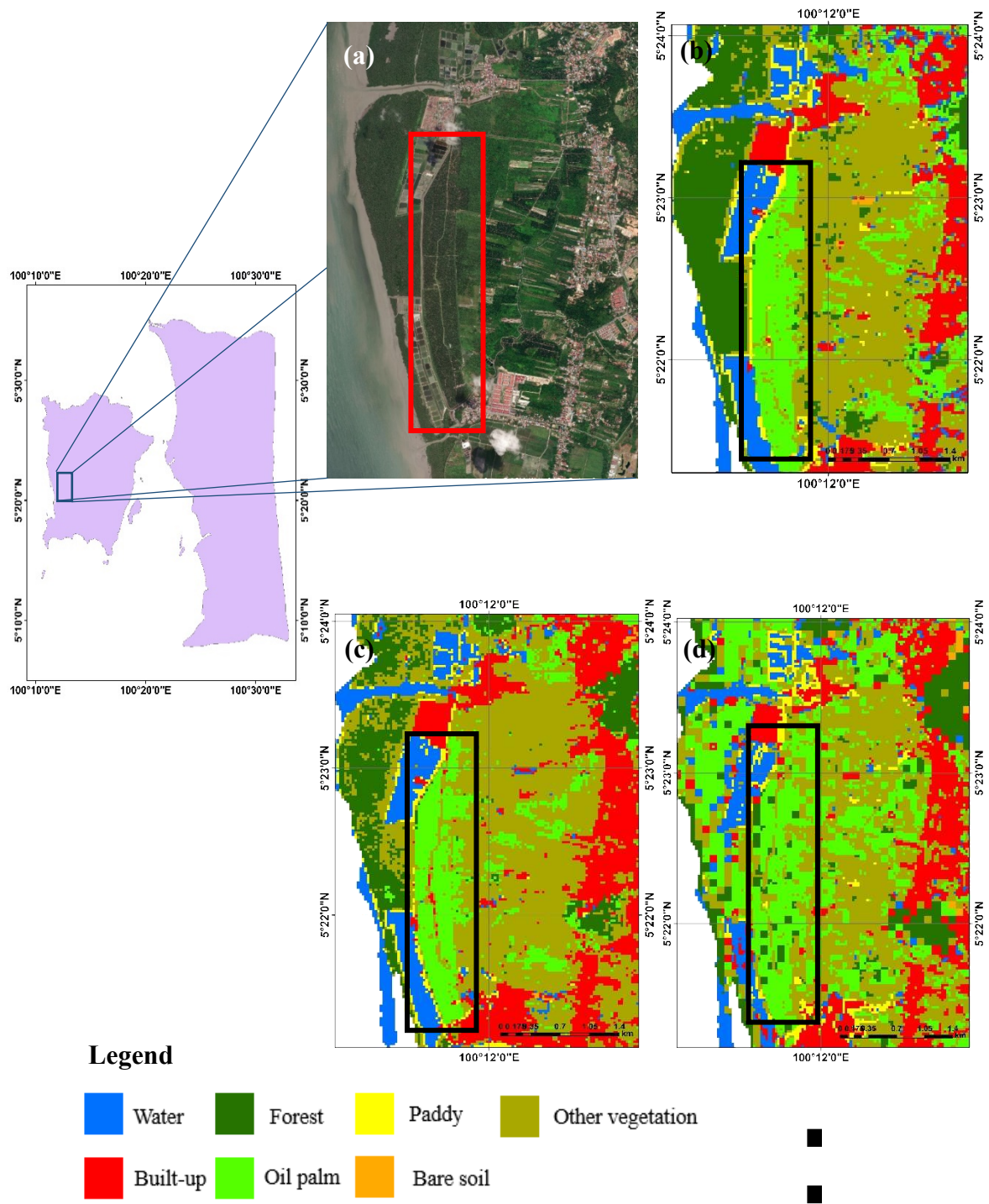


Figure 10. (a) High-resolution Google Earth image, (b) CART, (c) RF and (d) SVM.

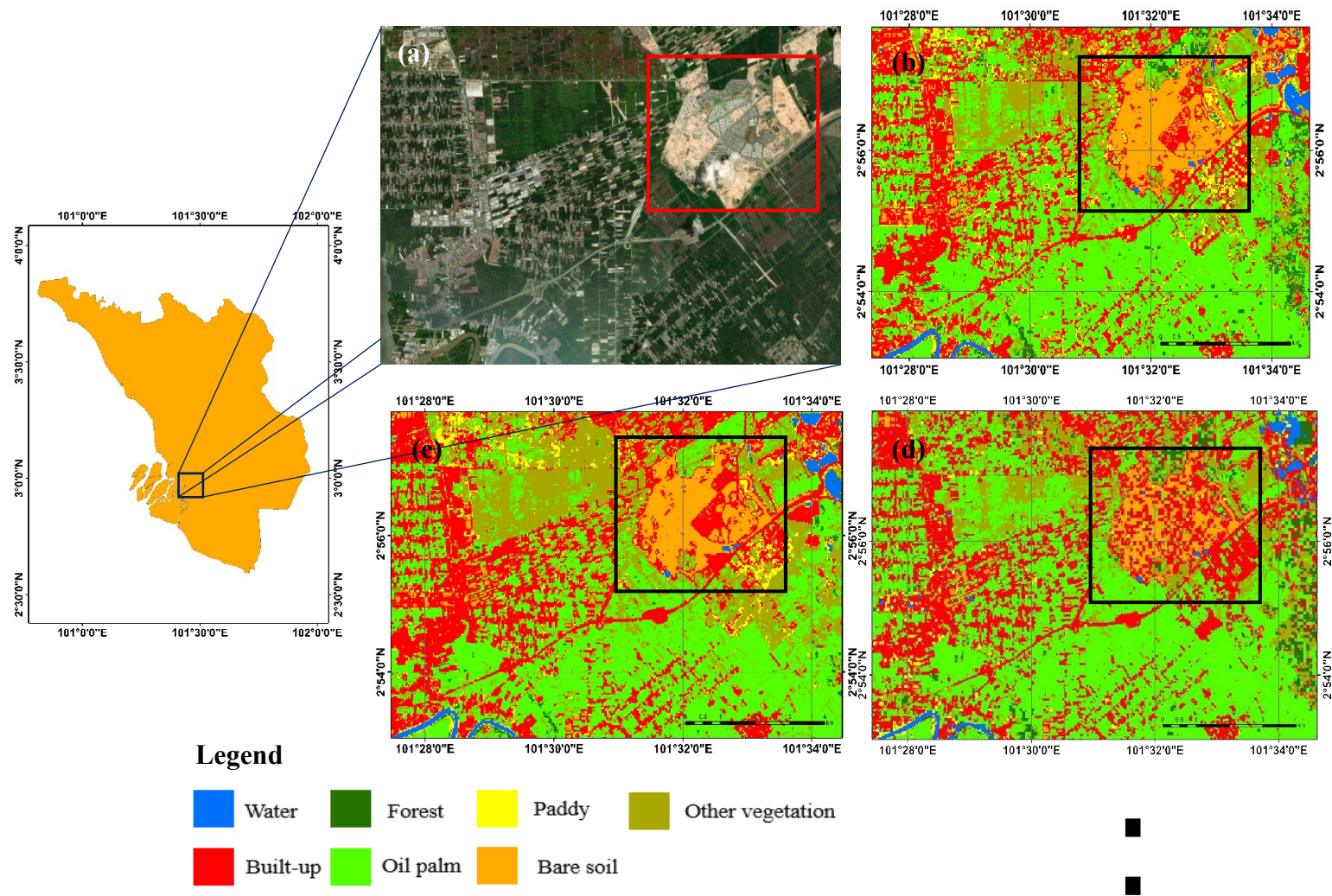


Figure 11. (a) High-resolution Google Earth image, (b) CART, (c) RF and (d) SVM.

Table 1. Information of the Landsat 8 bands.

Name	Description	Pixel size (m)	Wavelength (μm)
Band 1	Coastal aerosol	30	0.435 - 0.451
Band 2	Blue	30	0.452 - 0.512
Band 3	Green	30	0.533 - 0.590
Band 4	Red	30	0.636 - 0.673
Band 5	Near Infrared	30	0.851 - 0.879
Band 6	Short-wave Infrared 1	30	1.566 - 1.651
Band 7	Short-wave Infrared 2	30	2.107 - 2.294

Table 2. Additional layer to be included for classification.

Name	Formula	Reference/Source
NDVI	$\frac{NIR - Red}{NIR + Red}$	(Bannari et al., 1995; Maselli, 2004)
NDWI	$\frac{Green - NIR}{Green + NIR}$	(Xu et al., 2010)
Blue Red	$Blue - Red$	(Murray et al., 2018)
Blue Green	$Blue - Green$	

Table 3. Hyperparameters involved.

Algorithm	Hyperparameter
SVM	Kernel type = Radial Basis Function Gamma = 0.7 Penalty value = 10
CART	Cross validation factor = 5 Max depth = 10 Minimum leaf population = 5 Minimum split population = 10
RF	Number of trees = 30

Table 4. Overall, producer's and user's accuracies for oil palm class of each state and Peninsular Malaysia.

State		Johor	Kedah	Kelantan	Melaka	Negeri Sembilan	Pahang	Pulau Pinang	Perak	Perlis	Selangor	Terengganu	Peninsular Malaysia
RF	OA (%)	89.23	87.85	86.06	85.16	77.57	80.84	89.74	91.30	86.75	89.88	87.10	86.50
	PA (%)	84.62	100.00	89.66	92.00	68.75	80.49	93.10	81.82	85.71	92.45	87.50	86.92
	UA (%)	89.19	84.44	86.67	74.19	75.86	70.21	96.43	90.00	75.00	87.50	80.77	82.75
CART	OA (%)	82.74	86.74	73.94	87.50	78.04	76.64	80.13	82.61	69.88	78.75	83.87	80.08
	PA (%)	84.62	92.11	75.86	96.00	71.88	85.37	65.52	81.82	85.71	73.58	91.67	82.19
	UA (%)	76.74	85.37	73.33	80.00	58.97	70.00	65.52	81.82	50.00	88.64	59.46	71.82
SVM	OA (%)	89.38	97.35	98.18	88.28	88.32	81.28	96.15	97.10	97.59	97.62	93.55	93.16
	PA (%)	89.74	97.22	100.00	92.00	87.50	89.19	96.55	90.91	100.00	98.11	87.50	93.52
	UA (%)	85.37	97.22	93.55	82.14	80.00	76.74	96.55	90.91	100.00	96.30	91.30	90.01

Note: OA: Overall accuracy (7 classes); PA: Producer's accuracy (oil palm); UA: User's accuracy (oil palm)

Table 5. Oil palm area produced by RF, CART and SVM in comparison with MPOB.

State	Oil palm area (ha)						
	MPOB	RF		CART		SVM	
		Classified	Difference	Classified	Difference	Classified	Difference
Johor	748860	799142	50282	752133	3273	782282	33422
Kedah	87538	147744	60206	157801	70263	170060	82522
Kelantan	158310	126177	-32133	183388	25078	106969	-51341
Melaka	57372	45768	-11604	42186	-15186	46021	-11351
Negeri Sembilan	184815	184325	-490	195733	10918	194311	9496
Pahang	741495	720745	-20750	802325	60830	717739	-23756
Pulau Pinang	13563	13146	-417	16039	2476	16572	3009
Perak	406469	392518	-13951	445041	38572	528448	121979
Perlis	660	1779	1119	3760	3100	4789	4129
Selangor	137783	196807	59024	195375	57592	194506	56723
Terengganu	171548	167136	-4412	211977	40429	162737	-8811

Table 6. Contingency table.

	Test 2 (positive)	Test 2 (negative)	Row total
Test 1 (positive)	a	b	a + b
Test 1 (negative)	c	d	c + d
Column total	a + c	b + d	n

Table 7. McNemar's test result.

Algorithm 1	Algorithm 2	p-value
SVM	RF	0.28
SVM	CART	0.00
RF	CART	0.00

Conflict of Interest and Authorship Conformation Form

Please check the following as appropriate:

- All authors have participated in (a) conception and design, or analysis and interpretation of the data; (b) drafting the article or revising it critically for important intellectual content; and (c) approval of the final version.
- This manuscript has not been submitted to, nor is under review at, another journal or other publishing venue.
- The authors have no affiliation with any organization with a direct or indirect financial interest in the subject matter discussed in the manuscript
- The following authors have affiliations with organizations with direct or indirect financial interest in the subject matter discussed in the manuscript:

Author's name	Affiliation
Nur Shafira Nisa Shaharum	Department of Civil Engineering, Faculty of Engineering, Universiti Putra Malaysia, 43400, UPM Serdang, Selangor, Malaysia.
Helmi Zulhaidi Mohd Shafri	Department of Civil Engineering, Faculty of Engineering, Universiti Putra Malaysia, 43400, UPM Serdang, Selangor, Malaysia. Geospatial Information Science Research Centre (GISRC), Faculty of Engineering, Universiti Putra Malaysia (UPM), 43400 Serdang, Selangor, Malaysia.
Wan Azlina Wan Ab Karim Ghani	Department of Chemical and Environmental Engineering/Sustainable Process Engineering Research Centre (SPERC), Faculty of Engineering, Universiti Putra Malaysia, 43400, UPM Serdang, Selangor, Malaysia.
Sheila Samsatli	Department of Chemical Engineering, University of Bath, Claverton Down, BA2 7AY, United Kingdom.
Mohammed Mustafa Abdulrahman Al-Habshi	Department of Civil Engineering, Faculty of Engineering, Universiti Putra Malaysia, 43400, UPM Serdang, Selangor, Malaysia.
Badronnisa Yusuf	Department of Civil Engineering, Faculty of Engineering, Universiti Putra Malaysia, 43400, UPM Serdang, Selangor, Malaysia.

Ethical Statement for Remote Sensing Applications: Society and Environment

I testify on behalf of all co-authors that our article submitted to Solid State Ionics – Diffusion and Reactions:

Title: Oil Palm Mapping Over Peninsular Malaysia Using Google Earth Engine and Machine Learning Algorithms

All authors:

Nur Shafira Nisa Shaharum, Helmi Zulhaidi Mohd Shafri, Wan Azlina Wan Ab Karim Ghani, Sheila Samsatli, Mohammed Mustafa Abdulrahman Al-Habshi and Badronnisa Yusuf.

- 1) this material has not been published in whole or in part elsewhere;
- 2) the manuscript is not currently being considered for publication in another journal;
- 3) all authors have been personally and actively involved in substantive work leading to the manuscript, and will hold themselves jointly and individually responsible for its content.

Date: 3rd Oct 2019

Corresponding author's signature:



6 January 2020

Editor
Remote Sensing Applications: Society and Environment

Dear Sir,

SUBMISSION OF AN UPDATED MANUSCRIPT FOR CONSIDERATION OF PUBLICATION IN THE REMOTE SENSING APPLICATIONS: SOCIETY AND ENVIRONMENT JOURNAL

With reference to the matter as stated above, I would like to submit a manuscript entitled **“Oil Palm Mapping Over Peninsular Malaysia Using Google Earth Engine and Machine Learning Algorithms”** for consideration of publication in the Remote Sensing Applications: Society and Environment Journal. This paper requires improvements after being revised with the decision of minor correction.

We thank the editors and reviewers for the comments to help improve the quality of the manuscript. We have highlighted (using yellow highlighting with red font color) the changes made in our manuscript based on the comments.

The details on the response to the reviewers are given in the correction table for your reference and I hope it will receive a proper evaluation from the Journal reviewers and editors.

Best regards,



Helmi Zulhaidi Mohd Shafri
Dept. of Civil Engineering
UPM